

Structural and Magnetic Properties on Sr-substituted BiFeO₃ Perovskite Nanoferrites

Kaimin Su¹, Kangling Huang¹, Hu Yang^{1,*}, Yun He^{2,*}

¹College of Physics and Technology, Guangxi Normal University, Guilin 541004, China.

²Guangxi Key Laboratory of Nuclear Physics and Nuclear Technology, Guangxi Normal University, Guilin 541004, China.

*corresponding author

Keywords: Bi_{0.7}(Gd_{0.3-x}Sr_x)FeO₃, Sol-gel, Calcination temperature, M-H curves.

Abstract: This experiment using the method of polyacrylamide sol-gel synthetic Bi_{1-x}Sr_xFeO₃ (x=0.02~0.12) powder. The diffraction peak trend together with the increase of Sr²⁺ and the different calcining temperature show that the best calcining temperature is 600°C. The scanning electron microscope images that the reunion phenomenon more serious with the increase of doping and the particle morphology become more and more random. It can get smaller particle size with the increasing of Sr²⁺. Experimental results show that the minimum particle can be get when the calcining temperature is 600°C. With the increasing of Sr²⁺ ions, the area of hysteresis loop change distinct. When x=0.04, calcining temperature T=600°C can get a preferable particle.

1. Introduction

The materials which simultaneously exhibit two or more the basic performances of iron including ferromagnetic or anti-ferromagnetic, ferroelectricity and iron elastic is called multiferroic material that putting forward by Switzerland Schmid in 1994^[1]. Under certain temperature, this kind of materials presence spontaneous polarization and spontaneous magnetization simultaneously, which caused the magneto-electric coupling effect, this electric and magnetic mutual regulation caused several new and meaningful physical phenomena^[2-3]. Among the various investigated multiferroics, BiFeO₃ (BFO), with a rhombohedral distorted perovskite structure is the rare one which shows Weak ferroelectricity (830°C) and ferromagnetic (370°C) simultaneously at the room temperature^[4-6]. At present, the most popular application of the perovskite multiferroic material is in the solar cell. The method of preparing BiFeO₃ mainly about Hydrothermal method, Coprecipitation method^[7] and sol gel method^[8], etc. However, the pure phase of BiFeO₃ existence the delay of Fe³⁺ to Fe²⁺ due to the volatilize of Bi element in the process of preparation or the existence of oxygen vacancy, that cause leakage current^[9], making it difficult to get larger magnetoelectric. Many reports show that doping can inhibit the volatilization of Bi element which reduces the oxygen vacancies and improves the structure and the magnetoelectric. Currently, doping in A bit of BiFeO₃ is mainly by alkaline earth ions and rare earth ions. Alkaline earth metal ions as Ca^[10], Sr^[11], Ba^[12], rare earth ions as La, Nd, Sm, Gd, Dy. Doping in B bit of BiFeO₃ are mainly by excessive ions,

such as: Co, Ti, Mn, Nb, Cr, Sc, etc. In this present work, we use the Polyacrylamide sol-gel Route method which has the advantages of easy Control and convenient operation to synthetic BiFeO_3 nanoparticles that doping in A bit by Sr^{2+} .

2. Experiment Section and Synthesis

$\text{Bi}_{1-x}\text{Sr}_x\text{FeO}_3$ nanoparticles were prepared by a sol-gel auto-combustion method. The XRD, SEM and MPMS were used to investigate the microstructure and magnetic properties of $\text{Cu}_{0.7}\text{Zn}_{0.3}\text{Fe}_{2-x}\text{La}_x\text{O}_4$.

3. Results and Discussion

3.1. XRD Patterns and Structures Analysis

Figure 1 shows the X-ray diffraction pattern of the $\text{Bi}_{1-x}\text{Sr}_x\text{FeO}_3$ ($x=0.02\sim 0.12$) which calcined at 600°C for 3h and analyzed by jade 5 Software. As the increase of x value, the diffraction peak merge together, as (012), (110) merge into (110), (003), (021) merge into (021), (113), (211) merge into (211), etc. This suggests that the doping Sr^{2+} ions cause distortion of the crystal structure^[9, 10]. In addition, the half high width of the diffraction peak are becoming more and more wider with the increase of x value, with the increase of Sr^{2+} ions, crystal grain size are getting smaller^[11].

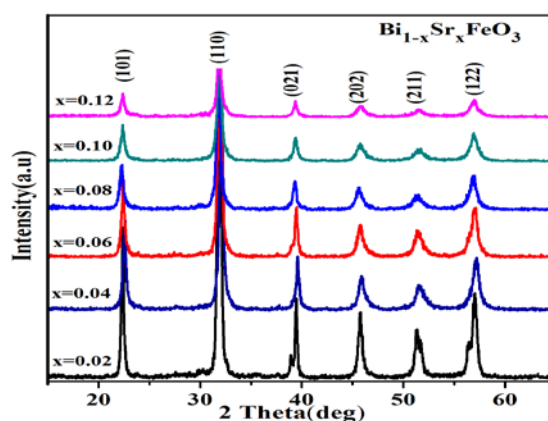


Figure 1: XRD of $\text{Bi}_{1-x}\text{Sr}_x\text{FeO}_3$ nanoparticles

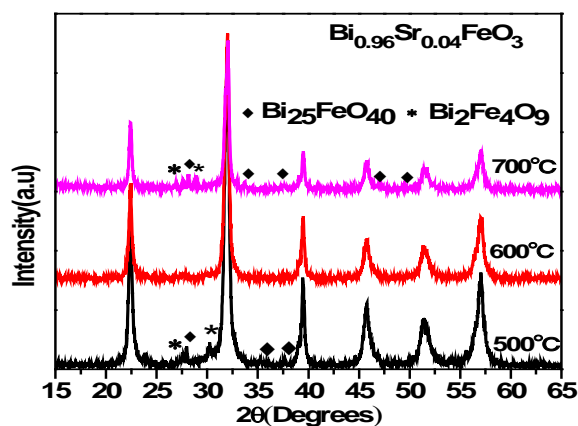


Figure 2: XRD of $\text{Bi}_{0.96}\text{Sr}_{0.04}\text{FeO}_3$ at different temperatures.

Figure 2 is XRD diagrams which calcining at different temperatures. With the calcining temperature from 500°C to 700°C, the diffraction peak of the sample is sharp with a well-crystallized. The $\text{Bi}_{25}\text{FeO}_{40}$ and $\text{Bi}_2\text{Fe}_4\text{O}_3$ mixed phase appear in $2\theta=25^\circ\text{-}40^\circ$ by calcining at 500°C, and when the calcining temperature up to 600°C, the two mixed phases disappeared, as calcining temperature continues to rise, the mixed phase increase, this phenomenon can be interpreted as:the sample is not fully reflect in Low calcining temperature that causing the appearance of the mixed phase. When the calcining temperature is 600°C, the second phases growth are inhibited, and didn't see the impurity phase^[12], continue to rise the calcining temperature, with the Bi^{3+} ion volatile cause oxygen vacancy and so on, making the mixed phase increased^[13-14].

3.2. Structures and grain size

The particle morphology from the scanning electron microscope images as shown in Figure 3, when the doping $x=0.04$, the particles shape are rectangular and clearly visible; with the increase of Sr^{2+} , particle shape becomes more and more random and difficult to discern.

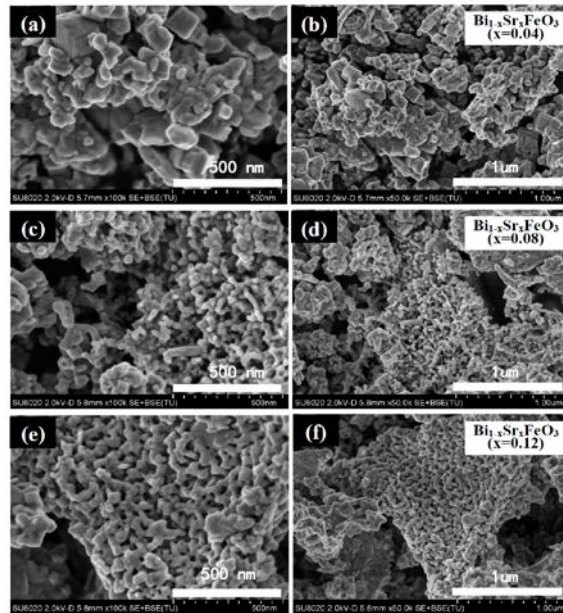


Figure 3: SEM of $\text{Bi}_{1-x}\text{Sr}_x\text{FeO}_3$ ($x=0.04, 0.08, 0.12$).

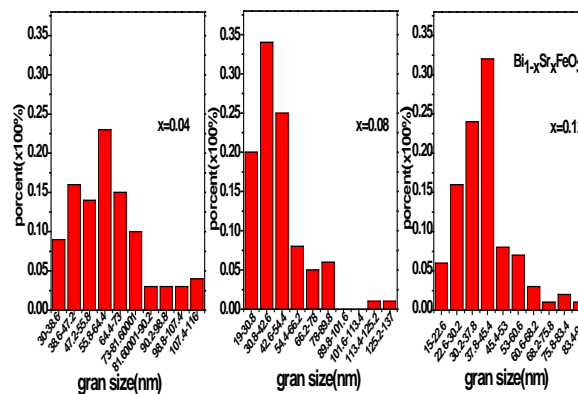


Figure 4: Size distribution of $\text{Bi}_{1-x}\text{Sr}_x\text{FeO}_3$.

In addition, with the increase of Sr^{2+} in the solution, the particle size of samples decreased greatly, especially from $x=0.04$ to $x=0.08$, when the doping is more than 0.08, the grain sizes decrease slow down, at the same time, reunion phenomenon of the sample also intensified, with the increase doping of Sr^{2+} , reduced the volatilize of Bi^{3+} which reduced oxygen vacancy, and decrease oxygen vacancy that did not conducive for the growth of $\text{Bi}_{1-x}\text{Sr}_x\text{FeO}_3$, making the particle morphology irregular and crystallization of incomplete, so that the particle size decrease^[34]; with the increase of Sr^{2+} , forces between particles increase, making the reunion more serious between particles. Figure 4 is the particle size distribution histogram of the samples. From the histogram, with the doping quantity increased of Sr^{2+} ions from 0.04 to 0.12, the particle size of sample all decreased, especially from 0.04 to 0.08, particle size decreases faster; when the dosage increased from 0.08 to 0.12, the decreasing slow down^[15].

Figure 5 reflected the scanning electron microscopy of the content of $x=0.04$ calcining temperature from 500°C to 700°C . According to the picture, calcining temperature has grade impact for the morphology of the sample. When calcining temperature is 500°C , samples showed larger particle sizes. As the calcining temperature up to 600°C , the particle size lower. When calcining temperature continues to rise to 700°C , particle size increased and reunion phenomenon also aggravating. By the available: when doping $x=0.04$, calcining temperature is 600°C , and get a better $\text{Bi}_{1-x}\text{Sr}_x\text{FeO}_3$ sample^[16].

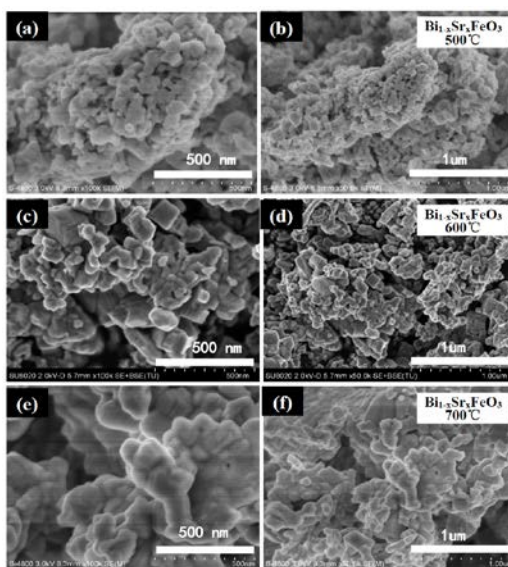


Figure 5: SEM of $\text{Bi}_{0.96}\text{Sr}_{0.04}\text{FeO}_3$ (500°C to 700°C).

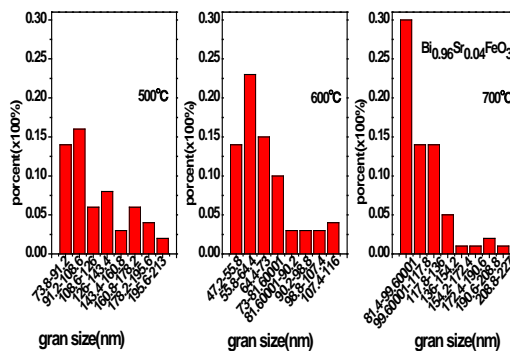


Figure 6: Size distribution of $\text{Bi}_{0.96}\text{Sr}_{0.04}\text{FeO}_3$.

Figure 6 is the particle size distribution histogram of the $\text{Bi}_{0.96}\text{Sr}_{0.04}\text{FeO}_3$ calcined at different temperatures. With the calcining temperature increasing, particle size of samples present the tendency of smaller before and increased follow. When calcining temperature is 500°C , more particles concentration in $73\sim 108$ nm and particle size distribution is more dispersed, as calcining temperature is 600°C , more particles relatively concentrated in $47\sim 73$ nm, and calcining temperature is 700°C , more concentration in $81\sim 136$ nm.

3.3. Magnetic Property of Particles

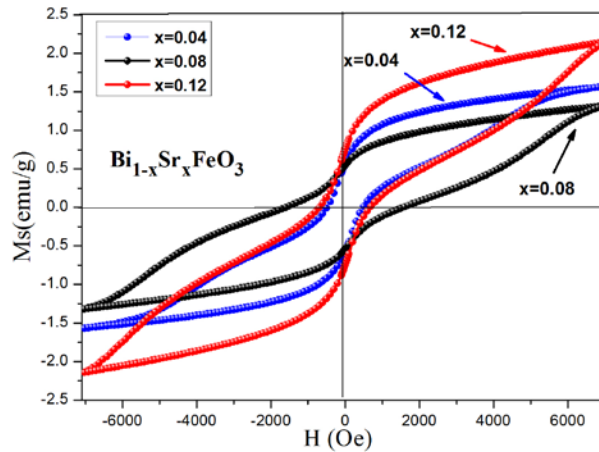


Figure 7: Hysteresis of $\text{Bi}_{1-x}\text{Sr}_x\text{FeO}_3$ ($x=0.04, 0.08, 0.12$) calcined at 600°C for 3h.

Figure 7 is given the hysteresis loop of $\text{Bi}_{1-x}\text{Sr}_x\text{FeO}_3$ which doping $x=0.04, 0.08, 0.12$ and calcining at 600°C for 3h. According to the shape of the curve, the three are not saturated state hysteresis loop, with the increase doping of Sr^{2+} , the area of loop increases, this is because: with the increase of Sr^{2+} , making the spiral structure of ferrite bismuth are destroyed more and more serious and release the greater magnetic^[35, 36]. The magnetic moment of Alkaline earth elements ions and ionic radius were the major causes for the saturated magnetization of the doped samples. Curve move in horizontal direction and vertical direction with the increase of Sr^{2+} .

Table 1: The hysteresis loop parameters of $\text{Bi}_{1-x}\text{Sr}_x\text{FeO}_3$.

Content(x)	M_S (emu/g)	H_C (Oe)	M_r (emu/g)	n_B
0.04	1.56824	501.9258	0.569305	0.086476
0.08	1.32048	1605.283	0.54552	0.071666
0.12	2.146995	702.0586	0.75617	0.114655

Table 1 shows the hysteresis loop parameters of $\text{Bi}_{1-x}\text{Sr}_x\text{FeO}_3$ calcined at 600°C for 3h. From the table, with Sr^{2+} doping increased from 0.04 to 0.12, the saturation magnetization (M_S) reduced from 1.56824 emu/g to 1.32048 emu/g and then increases to 2.146995 emu/g later, and the M_S change slower when the Sr^{2+} doping $x < 0.08$, as the doping $x \geq 0.08$, the M_S change quickly. the remanent magnetization (M_r) and n_B have the same change trends as the M_S . In the table, the large change is the coercive force (H_C), with the increase Sr^{2+} , the coercive force changes great and first increases then decreases. When the doping $x=0.08$, coercive force up to more than 1605 Oe.

4. Conclusion

This paper adopts the polypropylene sol-gel method to replace Bi^{3+} by Sr^{2+} , introducing chemical pressure by element substitution, thus changing the crystal structure of BiFeO_3 , then improving the structure, morphology, magnetic, etc. As replacing Bi^{3+} by Sr^{2+} , the system's structure was distorted due to the difference of the ionic radius. Different doping ratios of $\text{Bi}^{3+}/\text{Sr}^{2+}$ make the morphology different, and even at the same ratio, calcining at different temperatures, the morphology of the product is different. When doping $x=0.04$ and calcining at 600°C , we get better $\text{Bi}_{1-x}\text{Sr}_x\text{FeO}_3$ crystal morphology. Replacing by Sr^{2+} can effectively improve the magnetic of BiFeO_3 , the reason attributable to the special spiral magnetic structure damaged.

Acknowledgements

This work was financially supported by the National Natural Science Foundation of China (NO.12164006, 11364004) and Guangxi Key Laboratory of Nuclear Physics and Nuclear Technology. Kaimin Su and Kangling Huang contributed equally to this work. No potential conflict of interest was reported by the authors.

References

- [1] H. Schmid. *Multi-Ferroic Magnetolectrics*. *Ferroelectrics*. 1994, 162: 665-685.
- [2] J. D. Teague, R. Gerson, W. J. James. *Dielectric Hysteresis in Single Crystal BiFeO₃*. *Solid State Communications*. 1970, 8(13): 1073-1074.
- [3] F.M. Bai, J.L. Wang, M. Wuttig, J.F. Li, N.G. Wang, A.P. Pyatakov, A.K. Zvezdin, L.E. Cross, D. Viehland. *Destruction of Spin Cycloid in (111)c -Oriented BiFeO₃ Thin Films by Epitaxial Constraint: Enhanced Polarization and Release of Latent Magnetization*. *Applied Physics Letters*, 2005, 86(3): 32511.
- [4] F. Kubel, H. Schmid. *Structure of a Ferroelectric and Ferroelastic Mono-domain Crystal of the Perovskite BiFeO₃*. *Acta Crystallographica Section B: Structural Science*. 1990, 46(6): 698-702.
- [5] J. M. Moreau, C. Michel, R. Gerson, W. J. James. *Ferroelectric BiFeO₃ X-ray and Neutron Diffraction Study*. *Journal of Physics and Chemistry of Solids*. 1971, 32(6): 1315-1320.
- [6] C. Michel, J.M. Moreau, G. D. Achenbache, R. Gerson, W. J. James. *The Atomic Structure of BiFeO₃*. *Solid State Communications*. 1969, 7(9): 701-704.
- [7] C. Ederer, N. A. Spaldin. *Weak Ferromagnetism and Magnetolectric Coupling in Bismuth Ferrite*. *Physical Review B*. 2005, 71: 60401.
- [8] Jun Y K., Moon W.T, Chang C.M, et al. *Effects of Nb-doping on electric and magnetic properties in multiferroic BiFeO₃ceramics*. *solid state communications*, 2005, 135(1): 133-137.
- [9] J. D. Teague, R. Gerson, W. J. James. *Dielectric Hysteresis in Single Crystal BiFeO₃*. *Solid State Communications*. 1970, 8(13): 1073-1074.
- [10] R. Haumont, J. Kreisel, P. Bouvier. *Raman Scattering of the Model Multiferroic Oxide BiFeO₃: Effect of Temperature, Pressure and Stress*. *Phase Transitions*. 2006, 79(12): 1043-1064.
- [11] Jun Y K., Moon W.T, Chang C.M, et al. *Effects of Nb-doping on electric and magnetic properties in multiferroic BiFeO₃ceramics*. *solid state communications*, 2005, 135(1):133-137.
- [12] Zhao Q X, Zhang T, Ma J K et al. *Effect of Deposition Temperature on the Structural and Physical Properties of BiFeO₃ Films Prepared by Magnetron Sputtering*. *Journal of Synthetic Crystal*, 2011, 40(4) : 921-925.
- [13] V. A. Khomchenko, A. Kiselev, J. M. Vieira, and A. L. Kholkin. *Synthesis and multiferroic properties of Bi_{0.8}A_{0.2}FeO₃ (A=Ca,Sr,Pb) ceramics*. *Applied physics letters* 2007,90, 242901.
- [14] B Bhushan, A Basumallick, S K Bandopadhyay, N Y Vasanthacharya and D Das .*Effect of alkaline earth metal doping on thermal, optical, magnetic and Dielectric properties of BiFeO₃ nanoparticles*. *J. Phys. D: Appl. Phys.* 2009, 42, 65004.
- [15] K.F. Wang, J.M. Liu, Z.F. Ren. *Multiferroicity: the coupling between magnetic and polarization orders*. *Advances in Physics*, 2009, 58 (4): 321-448.
- [16] Wei Jie, Chen Yan-Jun, Xu Zhuo. *Study on the size-dependent magnetic properties of multiferroic BiFeO₃ nanoparticles*. *Acta Phys. Sin*, 2012, 61(5) 057502.